OECD/NEA CFD–UQ Benchmark Exercise:
CFD prediction and Uncertainty Quantification of a GEMIX mixing layer test

(Final version)

1. PRELIMINARY REMARKS

The present benchmark exercise on Uncertainty Quantification (UQ) in Computational Fluid Dynamics (CFD) constitutes the first of its kind worldwide. The main objective of this exercise is to compare and evaluate different UQ methodologies, currently used to assess the reliability of CFD simulations in the presence of several sources of uncertainties. The participants of this benchmark are free to choose the uncertainty sources (e.g. boundary conditions, turbulence model coefficients and numerical errors) and the methodology to compute uncertainty bands. The selection of numerical schemes, turbulence models and computational mesh are also left to participants' discretion. The selected test facility for the benchmark is GEMIX (**GE**neric **MI**xing e**X**periment), developed at the Paul Scherrer Institute in Switzerland.

2. EXPERIMENTAL TEST SECTION

The confined wake flow water mixing experiments in the GEMIX facility, focus on the basic turbulent mixing mechanisms for unstratified and stably stratified conditions. A simplified schematic of the test rig is shown in Fig. 1. The flow channel is made of acrylic glass to enable optical access, except for the last 80mm of the splitter plate, which is made of stainless steel to avoid deformation of the splitter plate tip. The main design parameters for the GEMIX flow channel are listed in Table 1. The coordinate system to describe the velocity and concentration fields is located at the tip of the splitter plate and its origin is placed in the middle of the channel. The x-coordinate represents the streamwise direction, the y-coordinate the crosswise and the z-coordinate the spanwise direction (see Fig. 1).

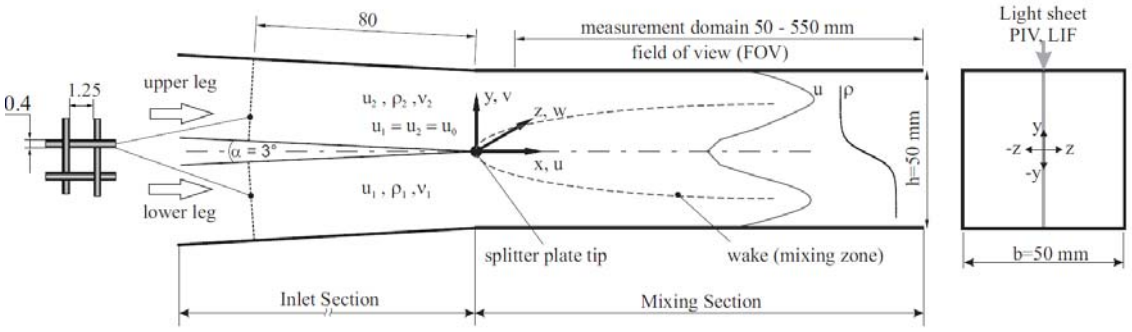

Figure 1. Schematic of the GEMIX test rig.

The inlet section comprises the lower and upper legs, where the two co-flowing water streams are initially separated by the splitter plate. Upper and lower legs are equipped with flow conditioning devices, where both streams pass through a single honeycomb, two identical coarse grids and a single fine grid, such that the velocity profiles at the splitter plate tip appear almost equal in shape and free from rotational components. The wire diameter *d*, mesh width *w* and upstream location of the braided flow conditioning grids as well as the diameter *d*, length *l* and rear edge position of the circular cell honeycombs are listed in Table 1. For the experiments, each leg of the inlet section is supplied with the same volumetric flow rate from an individual pumping line connected to its own individual water storage tank of 2000 l capacity, enabling separate conditioning for each stream. One storage tank contains tap water, while the other one contains either de-ionized water or a solution of de-ionized water and sucrose to increase the density of the lower stream to establish stable stratified flow conditions. Sucrose is used to increase the density of the lower stream instead of salt, because it makes only minor changes to the electrical conductance of the water, which is important for using the wire-mesh sensor with its measurement principle—based on electrical conductivity—unaltered. The mass fraction of sucrose in conjunction with a temperature adjustment is used to alter the density differences between the streams while

keeping the kinematic viscosity (and therefore the Reynolds Numbers Re_0) of the two streams approximately identical to that of pure water at 1 bar, 20°C (see table 2).

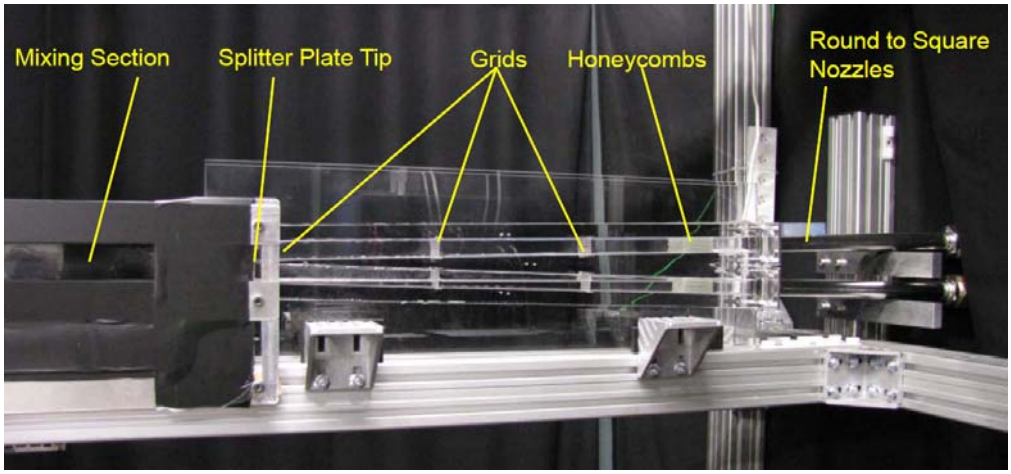

Figure 2. Inlet conditioning section.

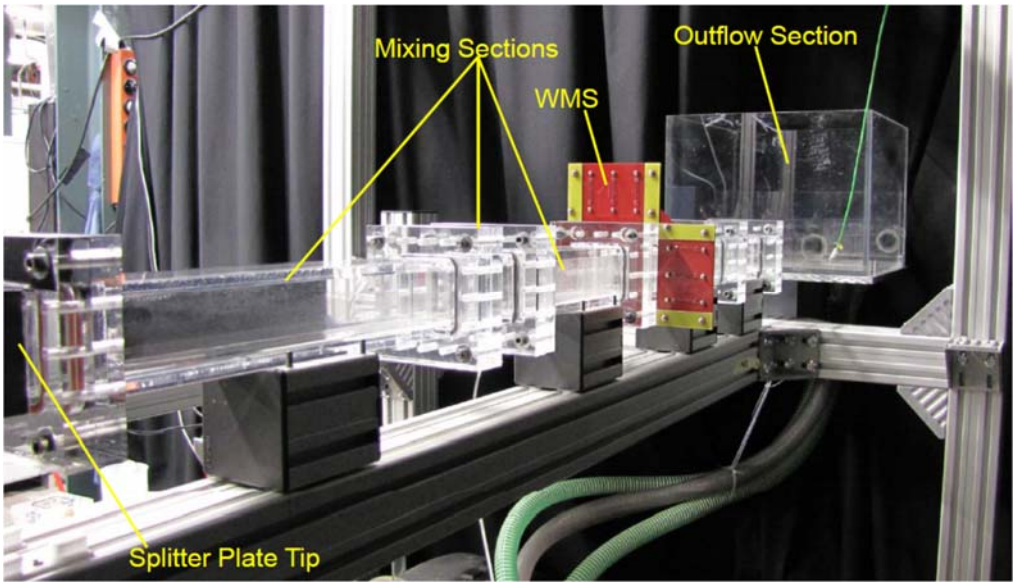

Figure 3. Mixing section.

The mixing section assembly, in which both streams interact and form the wake mixing zone past the splitter plate tip, is attached to the inlet section. The square mixing section is composed by non-adjustable walls with a cross-sectional area of 50×50 mm^2 and a length of 550 mm. The mixing section can be assembled by a single segment of 550 mm in length when PIV or LIF is applied to measure the mixing process, or by two segments of different length in order to place a wire-mesh sensor in the cross sectional area at various downstream distances. Only one wire-mesh sensor is placed in the mixing section; therefore, to measure cross-sectional concentration profiles at several locations, different experiments are needed (one per each location of the wire-mesh sensor). The outlet section is aligned to the mixing section and consists of an additional straight channel segment of 1 m in length, a flow splitter device and a water box with a spillover weir. At the end of the additional straight channel segment, the flow is split again into two streams in order to minimize possible feedback effects of the water box to the developing wake flow upstream. The rectangular water box has a volume of 40 *l* and a spillover weir that maintains constant back pressure of 250 mm head in the channel for all flow rates. The mass flow rates,

densities and temperatures of the two streams are recorded for each experimental run and the measured data is stored and processed on a computer.

Table 1. Main design parameters of the GEMIX flow channel (geometric dimension in mm). The flow conditions correspond to those in the full experimental campaign.

Inlet section length	1250
Inlet section height × width	25×50 (2×)
Splitter plate angle	3˚
Honeycomb d = 2, l = 50	@ x = -670
1. Grid d = 1, w = 4	@ x = -520
2. Grid d = 1, w = 4	@ x = -300
3. Grid d = 0.4, w = 1.25	@ x = -80
Mixing section length	550
Mixing section height × width	50×50
Total channel length	3000
Nominal inlet velocities	0.2-1.2 m/s
Re-Numbers in mixing section	10,000 – 60,000
Volumetric flow rate	15 – 90 l/min
Density difference	0 – 10%
Temperature difference	0 – 50K
Viscosity difference	0 – 100%
Streamwise turbulence level	≈ 5%

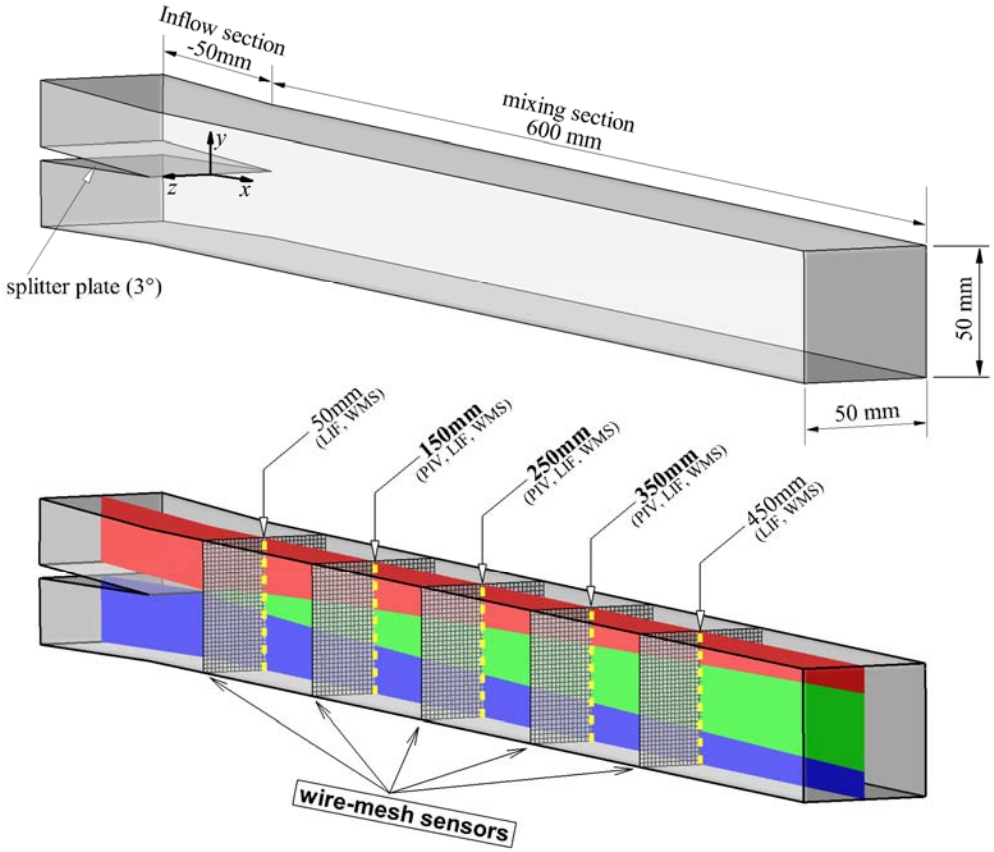

Figure 4. Schematic of GEMIX. Geometrical information of the CFD domain is provided in the top image. Comparison between simulations and experimental results will be carried out using several profiles at the center plane of the mixing section.

.

3. EXPERIMENTAL UNCERTAINTIES

The accuracy of volumetric flow rate—as monitored by the Coriolis flow meters—was ±0.15%. The error associated to the density measurement was estimated to be ±0.01 kg/m^3. The relative difference between the volumetric flows in the upper and lower legs of the inlet section, which determines the accuracy of the isokinetic condition $u_0 = u_1 = u_2$, was kept below $(\dot{V}_1 - \dot{V}_2)/\dot{V}_1 \cdot 100 \leq \pm 1\%$ for all the experiments.

Since we can only measure estimators for mean and RMS values from the experimental data (PIV, LDA and LIF), a quantification of the statistical uncertainty associated to these estimators is required. Thus, the mean and RMS values provided in the experimental data files have a level of uncertainty, characterized by an interval of confidence. For mean values, the interval of confidence was determined from the Student's distribution [1], while for RMS values, a nonparametric X^2-test [1,2] was applied. Since the Student's distribution is symmetric, the upper and lower bands—corresponding to the 95% interval of confidence—are also symmetric. However, the X^2distribution is not symmetric and therefore the upper and lower bands are slightly asymmetric respect to RMS value. The uncertainty for the turbulence kinetic energy was estimated by combining the individual uncertainties of the diagonal components of the Reynolds stress tensor, that is

$$\Delta k = \sqrt{U_1^2 + U_2^2 + U_3^2}, \tag{4}$$

where each uncertainty was calculated as

$$U_1 = \frac{\partial k}{\partial \langle u'u' \rangle} \cdot \sigma(\langle u'u' \rangle), \;\; U_2 = \frac{\partial k}{\partial \langle v'v' \rangle} \cdot \sigma(\langle v'v' \rangle), \;\; U_3 = \frac{\partial k}{\partial \langle w'w' \rangle} \cdot \sigma(\langle w'w' \rangle). \tag{5}$$

On locations where **only** the x- and y-components of the velocity could be measured (i.e. all PIV results and some LDA results), we assume the spanwise z-component to be equal to the vertical velocity component:

$$\Delta k = \sqrt{U_1^2 + 2 \cdot U_2^2} \tag{6}$$

In addition to the statistical uncertainty, the Signal to Noise Ratio (SNR) introduces additional uncertainties to the LIF measurements of the concentration field. The SNR and statistical uncertainties were combined into a single value for LIF data. Wire Mesh Sensor (WMS) data have been discarded for the present benchmark, because its associated uncertainty has not been fully clarified.

4. EXPERIMENTAL TEST MATRIX

The complete campaign in the GEMIX facility comprises experimental conditions with inlet mean velocities ranging from 0.2 to 1 m/s and density ratios of 0 to 10%, leading to a total of thirty independent cases. Nonetheless, for this benchmark exercise only four experiments will be considered—three will be disclosed and one will be kept secret for the blind calculations.

Table 2. Experimental matrix for this benchmark.

Inlet mean velocity	0.6 m/s	1 m/s
Global Re-number	30000	50000
Δρ = 0%, ΔT = 0K	N339	N337
Δρ = 1%, ΔT = 2.5K	N320	**N318**

The selected experiment for the blind calculation is N318. Inlet boundary conditions will be provided for all the experiments. However, velocity, Reynolds stresses (*u'u', u'v', v'v'*) and concentration profiles inside the mixing section—at the locations shown in Fig. 4—will be provided only for the other three cases. These data can be used freely by the participants, for instance, to calibrate physical models, mesh improvement or to obtain the uncertainty band in extrapolation methods.

5. PHYSICAL PROPERTIES

The physical properties of water for the experiments considered in this benchmark exercise are listed in table 3.

Properties of de-ionized as well as tap water were considered identical.

Table 3. Physical properties for tap/de-ionized water and for the mixture de-ionized water + sucrose 2.7 wt%.

	Tap / de-ionized water @ 20C	De-ionized water + sucrose @ 22.5C
$k\left(W/mK\right)$	0.6	0.6
$Cp\left(kJ/kgK\right)$	4.18	4.18
$\rho\left(kg/m^3\right)$	998	1008
$\mu\left(N/m^2s\right)$	1.002	0.991

6. MEASURING THE INLET BOUNDARY CONDITIONS

Mean velocities and their associated fluctuations were measured—with Laser Doppler Anemometry (LDA)—in one quadrant of the upper leg 50 mm upstream the tip of the splitter plate (see Fig. 5). Figure 6, shows the location of the measuring points for the inlet boundary condition. Due to limitations in optical access, the three velocity components could only be measured at the locations marked in pink. The black markers correspond to the location were only two velocity components were measured (x,y). Hence, in the data files for the inlet boundary conditions, the RMS values of the z-component were filled with zeros for those locations.

To construct the whole upper leg inlet boundary condition, symmetry was assumed among the four quadrants. Because the Reynolds number for both legs is the same (even for a $\Delta\rho$ = 1%), the inlet boundary condition for the lower leg was obtained by applying symmetry once again along the z-coordinate. Since LDA measurements at each point are time consuming, it was decided to measure only the upper leg. The distribution of the measuring points in the cross sectional area of the conditioning section is shown in Fig. 6. The experiments were performed at room temperature and, therefore, heat losses can be considered negligible, even for the case with $\Delta\rho$ = 1% where the temperature in the lower leg is slightly higher (2.5°C) than that of the upper leg.

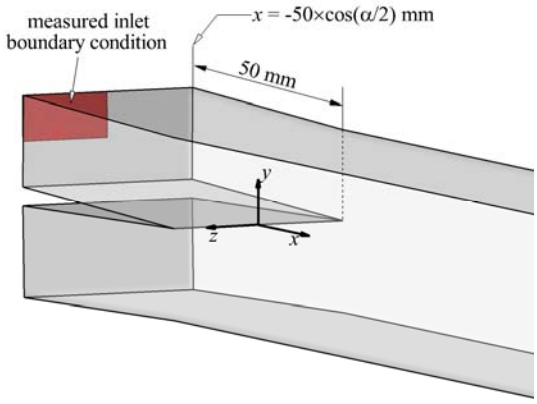

Figure 5. Location of the LDA measurement plane. These measurements were used to determine the inlet boundary condition for the CFD simulations.

It is important to remark the LDA measuring plane for inlet boundary condition was inclined 1.5deg respect to the yz-plane to obtain a streamwise velocity profile parallel to the surface of the splitter plate, hence, the x-coordinate of the measuring points changes slightly for each value of the y-coordinate. The files containing the experimental measurements of the inlet boundary conditions have the proper coordinates in the xyz Cartesian system. The time averaged velocity at each point was calculated according to:

$$\bar{u} = \frac{1}{N}\sum_{i=1}^{N} u_i, \tag{1}$$

where N correspond to the total number of samples and u_i is the instantaneous velocity at a given point. The root mean square (R.M.S.) of velocity fluctuations was calculated by:

$$\langle u' \rangle_{RMS} = \sqrt{\frac{1}{N-1}\sum_{i=1}^{N}(u_i - \bar{u})^2} \tag{2}$$

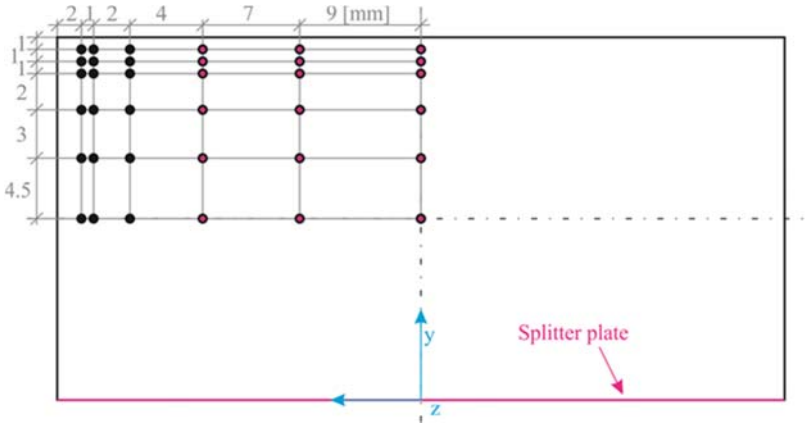

Figure 6. Location of the measuring points for velocity inlet boundary conditions with LDA.

Since the available LDA system enables for one-dimensional pointwise measurements of the instantaneous velocities, the three components of the velocity fluctuations cannot be measured simultaneously. Hence, the three components of the velocity fluctuations were measured by re-orienting the LDA system in different directions. For the points where the three velocity components were measured (pink markers in Fig. 6), the turbulence kinetic energy was calculated according to:

$$k = \frac{1}{2}\left(\langle u' \rangle_{RMS} + \langle v' \rangle_{RMS} + \langle w' \rangle_{RMS}\right) \tag{3}$$

For the locations where only two velocity components are available (black markers in Fig. 6), the turbulence kinetic energy is obtained by

$$k = \frac{1}{2}\left(\langle u' \rangle_{RMS} + 2\langle v' \rangle_{RMS}\right) \tag{4}$$

The mean velocity profile obtained from the LDA measurements at the inlet of the CFD domain is presented in Fig. 7. This figure also shows the location of the measuring points. Points located at the walls were assigned with null values.

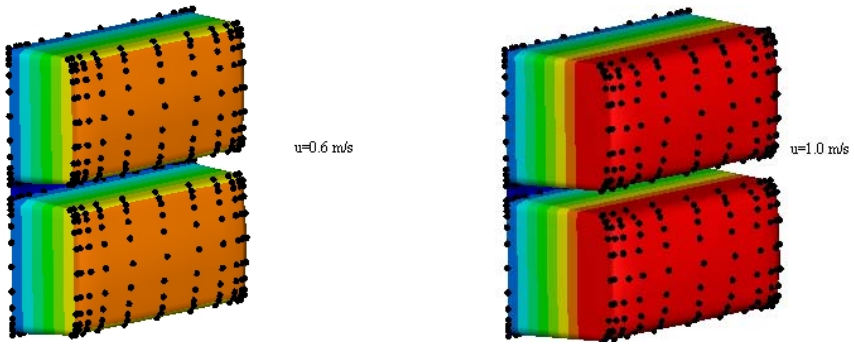

Figure 7. LDA mean velocity profiles at the inlet of the CFD domain (50 mm behind the tip of the splitter plate).

Because the Reynolds number was the same for $\Delta\rho$ = 0% and $\Delta\rho$ = 1%, the velocity profiles and turbulence quantities are assumed to be equal for these two cases.

7. DATA FILES AND FORMATS

The names of the files containing the experimental data for the inlet velocity measurements are given in table 4. The files start with header lines including the file name and variables (TecPlot format), that is

```
TITLE = "Vel_Inlet_X-50_u06ms.dat"
VARIABLES = "x", "y", "z", "Vx", "U_x95", "Vy", "U_y95", "Vz", "U_z95", "RMSVx",
            "RMSVxUpper", "RMSVxLower", "RMSVy", "RMSVyUpper", "RMSVyLower",
            "RMSVz", "RMSVzUpper", "RMSVzLower", "k", "kLOWER", "kUPPER"
ZONE T="Frame 1" I = 26  J = 13  F=POINT
```

The experimental data points are given after the header lines. The first three columns contain the coordinates (x,y,z). The 4th column is dedicated to the mean velocity in the streamwise direction (parallel to the splitter plate and normal to the measuring plane), followed by the corresponding uncertainty in column 5[1]. The 6th and 7th columns contain the mean velocity in vertical direction and the corresponding uncertainty, respectively. The 8th and 9th columns contain the mean velocity in spanwise direction and the corresponding uncertainty, respectively. Column 10 contains the R.M.S. value of the velocity fluctuations in streamwise direction with the appropriate lower and upper bound of the statistical uncertainty in columns 11 and 12. Column 13 contains the R.M.S. value of the velocity fluctuations in vertical direction with the appropriate lower and upper bound of the statistical uncertainty in columns 14 and 15. Column 16 contains the R.M.S. value of the velocity fluctuations in spanwise direction with the appropriate lower and upper bound of the statistical uncertainty in columns 17 and 18. Column 19 contains the Turbulent Kinetic Energy with the appropriate lower and upper bound of the statistical uncertainty in columns 20 and 21.

Table 4. Nomenclature used for the data files of the inlet velocity measurements.

position	Nominal velocity	File name
X=-50mm	1.0 m/s	`Vel_Inlet_X-50_u10ms.dat`
X=-50mm	0.6 m/s	`Vel_Inlet_X-50_u06ms.dat`

Since the measuring points will most likely not coincide with the computational mesh, the participants are free to use the experimental inlet measurements in the way that suits best their computational setup. For example, some participants may choose to use non-uniform rational B-splines (NURBS) interpolating surfaces, while others, may simply use a linear interpolation.

The names of the files containing the experimental data for the PIV measurements inside the mixing section are presented in table 5. The data is organized as follows: the files start header lines including the file name and variables, that is

```
TITLE = "X450_PIV_dr1_u06.dat"
VARIABLES = "x", "y", "Vx", "U_x95", "Vy", "U_y95", "RMSVx", "RMSxLOW", "RMSxUP", "RM
SVy", "RMSyLOW", "RMSyUP", "tauxy", "tauxyLOW", "tauxyUP", "k", "kLOW", "kUP"
ZONE I = 18
```

The experimental data points are given after the three header lines. The first two columns contain the coordinates (x,y). The 3rd column is dedicated to the mean velocity in the streamwise direction (parallel to the splitter plate and normal to the measuring plane). The 4th column contains the statistical uncertainty with a significance interval of 95%. The 5th column contains the mean velocity in vertical direction and the 6th column the corresponding uncertainty, again with an interval of confidence of 95%. The 7th column contains the streamwise velocity fluctuations. The lower and upper bound of the uncertainties regarding the streamwise velocity fluctuations are given in columns 8 and 9, respectively. The 10th column contains the vertical velocity fluctuations. The lower and upper bound of the uncertainties regarding the vertical velocity fluctuations are given in columns 11 and 12, respectively. The 13th column contains the covariance term $\langle u'v' \rangle$ and its

[1] It is important to mention that for all RMS values—including the turbulence kinetic energy—the uncertainty is given in the form of upper and lower uncertainty bands (mean ± uncertainty), whereas for mean values, only the uncertainty is provided.

associated lower and upper bands are given in the 14th and 15th columns respectively. The 16th column contains the turbulent kinetic energy. The lower and upper bound of the turbulent kinetic energy are given in columns 17th and 18th respectively.

Table 5. Nomenclature used for the data files of the PIV measurements.

Position / mm	Nominal velocity	Density ratio	File name	Experiment
X = 50mm	0.6 m/s	0.0%	X050_PIV_dr0_u06.dat	N339
X = 150mm	0.6 m/s	0.0%	X150_PIV_dr0_u06.dat	
X = 250mm	0.6 m/s	0.0%	X250_PIV_dr0_u06.dat	
X = 350mm	0.6 m/s	0.0%	X350_PIV_dr0_u06.dat	
X = 450mm	0.6 m/s	0.0%	X450_PIV_dr0_u06.dat	
X = 50mm	0.6 m/s	1.0%	X050_PIV_dr1_u06.dat	N320
X = 150mm	0.6 m/s	1.0%	X150_PIV_dr1_u06.dat	
X = 250mm	0.6 m/s	1.0%	X250_PIV_dr1_u06.dat	
X = 350mm	0.6 m/s	1.0%	X350_PIV_dr1_u06.dat	
X = 450mm	0.6 m/s	1.0%	X450_PIV_dr1_u06.dat	
X = 50mm	1.0 m/s	0.0%	X050_PIV_dr0_u10.dat	N337
X = 150mm	1.0 m/s	0.0%	X150_PIV_dr0_u10.dat	
X = 250mm	1.0 m/s	0.0%	X250_PIV_dr0_u10.dat	
X = 350mm	1.0 m/s	0.0%	X350_PIV_dr0_u10.dat	
X = 450mm	1.0 m/s	0.0%	X450_PIV_dr0_u10.dat	

The names of the files containing the experimental data for the LIF measurements in the mixing section are presented in table 6. The data is organized as follows: the files start with three text lines including the file nale and variables, that is

```
VARIABLES = "y", "c", "c_95","c'","c'low","c'high"
ZONE
DT=(DOUBLE,DOUBLE,DOUBLE,DOUBLE,DOUBLE,DOUBLE,DOUBLE,DOUBLE)
```

The experimental data points are given after the three header lines. The 1st column contains the y-coordinate. The 2nd column contains the mean concentration followed by the statistical uncertainty of the mean concentration with 95% significance level in the third column. The 4th column contains the species concentration fluctuation and the corresponding lower and upper bounds of the uncertainty associated with the concentration fluctuations are given in columns 5 and 6, respectively.

Table 6. Nomenclature used for the data files of the LIF measurements.

Position / mm	Nominal velocity	Density ratio	File name	Experiment
X = 50mm	0.6 m/s	0.0%	X050_LIF_dr0_u06.dat	N339
X = 150mm	0.6 m/s	0.0%	X150_LIF_dr0_u06.dat	
X = 250mm	0.6 m/s	0.0%	X250_LIF_dr0_u06.dat	
X = 350mm	0.6 m/s	0.0%	X350_LIF_dr0_u06.dat	
X = 450mm	0.6 m/s	0.0%	X450_LIF_dr0_u06.dat	
X = 50mm	0.6 m/s	1.0%	X050_LIF_dr1_u06.dat	N320
X = 150mm	0.6 m/s	1.0%	X150_LIF_dr1_u06.dat	
X = 250mm	0.6 m/s	1.0%	X250_LIF_dr1_u06.dat	
X = 350mm	0.6 m/s	1.0%	X350_LIF_dr1_u06.dat	
X = 450mm	0.6 m/s	1.0%	X450_LIF_dr1_u06.dat	
X = 50mm	1.0 m/s	0.0%	X050_LIF_dr0_u10.dat	N337
X = 150mm	1.0 m/s	0.0%	X150_LIF_dr0_u10.dat	
X = 250mm	1.0 m/s	0.0%	X250_LIF_dr0_u10.dat	
X = 350mm	1.0 m/s	0.0%	X350_LIF_dr0_u10.dat	
X = 450mm	1.0 m/s	0.0%	X450_LIF_dr0_u10.dat	

Since the measuring points will most likely not coincide with the computational mesh, the participants are free to use the experimental inlet measurements in the way that suits best their computational setup. For example, some participants may choose to use non-uniform rational B-splines (NURBS) interpolating surfaces, while others, may simple use a linear interpolation.

8. BASIC INFORMATION OF THE NUMERICAL SOLUTION

We request the following information concerning the physical/numerical solution procedure for each CFD simulation:

1. Code used, including version number
2. Total number of control volumes employed
3. Order of the spatial differencing scheme and type (e.g. 2nd-order upwind)
4. Convergence criteria
5. Water self-diffusion coefficient
6. Turbulence model (e.g. none, standard k-ε, LES (Smagorinsky), etc.)
7. Wall treatment (e.g. wall-resolved, wall functions, van Driest damping, etc.)
8. Total CPU time required for the blind calculation (summation from all processors), including all the simulations needed for the computation of the uncertainty bands. For example, if the calculation of the blind case—including the determination of the uncertainty bands—requires 20 CFD runs using 8 cores each, the total CPU time will be $20 \times 8 \times \sum t_i$, where t_i correspond to the CPU time in the i-th run
9. Total number of simulations needed to compute the uncertainty bands for the blind calculation
10. The name of the method employed for the quantification of uncertainties
11. Method for mapping the experimental inlet boundary condition onto the computational grid

This information is to be supplied in an ASCII file, named *Userxx_Information.dat*. The format of the file is presented below.

Userxxx

Item	**Short description**	**Information**
1	Code used	ANSYS Fluent, V14.0
2	Control volumes	450000
…		
9	Total number of simulations needed to…	20
11	…	

9. NUMERICAL DATA REQUESTED

For this exercise the participants are requested to provide mean velocity, turbulence kinetic energy and concentration profiles along the y-coordinate at selected locations inside the mixing section. The locations along the x-coordinate—where profiles must be provided—are shown in Fig. 4. The file format and y-coordinate of the points composing the profiles are identical to those in the experimental files provided by PSI (table 5). Thus, the participants are encouraged to rename and modify one of those files and replace the experimental values with their calculations. The participants are requested to submit individual files for each profile and name them accordingly to their x-location, that is, *Userxx_UQ_x_0.05.dat, Userxx_UQ_x_0.15.dat, Userxx_UQ_x_0.25.dat, Userxx_UQ_x_035.dat, Userxx_UQ_x_0.45.dat.* All files at the five locations must conform to the following format

Userxxx

x	**y**	**U**	**U-DU**	**U+DU**	**K**	**K-DK**	**K+DK**	**C**	**C-DC**	**C+DC**
0.05	-0.025	0.6	0.5	0.7	0.1	0.09	0.11	0.1	0.09	0.11
0.05	-0.024	0.6	0.5	0.7	0.1	0.09	0.11	0.1	0.09	0.11
...										

The first line must contain the user-ID (to be provided by PSI). The columns correspond to **x-coord(m)**, **y-coord(m)**, mean velocity in the stream wise direction **U(m/s)**, lower uncertainty band for the mean velocity **U-DU(m/s)**, upper uncertainty band for the mean velocity **U+DU(m)**, turbulence kinetic energy **K(m/s)²**, lower uncertainty band for turbulence kinetic energy **K-DK(m/s)²**, upper uncertainty band for turbulence kinetic energy **K+DK(m/s)²**, normalized concentration **C(dimensionless)**, lower uncertainty band for concentration **C-DC(dimensionless)**, upper uncertainty band for concentration **C+DC(dimensionless)**. This data will be used to compare the simulations with experiments and rank the submissions according to a set of measures that will be explained in the next section.

An **optional** sensitivity analysis is requested from the participants. The additional files including the results of the sensitivity analysis, should comply with the following rules: Depending on the number of uncertainty sources, these files will contain a different number of columns. Similar to the files containing the CFD simulations (plus uncertainty bands), these files must include profiles of the sensitivity coefficients for each uncertain parameter at the same five locations displayed in Fig. 4. Each grid point along the five profiles should be considered as an independent system, and therefore, the distribution of the sensitivity coefficients will change along the y-coordinate. These files should be named *Userxx_SA_x_0.05.dat, Userxx_SA_x_0.15.dat, Userxx_SA_x_0.25.dat, Userxx_SA_x_0.35.dat, Userxx_SA_x_0.45.dat.* The format is as follows

Userxxx

x	y	S1	S2	S3	S4	...
0.05	-0.025	0.6	0.1	0.1	0.1	...
0.05	-0.024	0.6	0.1	0.1	0.1	...
...						

The first two columns contain the location of the points where the sensitivity coefficients are calculated (profiles taken along the yellows lines in Fig. 4). The subsequent columns contain the sensitivity coefficient for each uncertain parameter (e.g. if the system has four uncertain variables or parameters, the participant should include the sensitivity coefficient for each of them in a separate column). A sensitivity analysis is fundamental in any UQ analysis to determine what are the variables or parameters introducing the highest uncertainty to the CFD results. This information will not be used in the ranking elaboration, but it is vital to elucidate the difference and capabilities of the different UQ methods. Each participant will most likely calculate the sensitivity coefficients in each grid point along the y-coordinate for the five x-locations, but since the CFD mesh does not necessarily coincide with points requested in the files *Userxx_SA_*.dat,* the participant are required to use a linear interpolation for calculating the sensitivity coefficients at the proper y-locations.

10. SHORT DESCRIPTION OF THE UQ METHOD

The participants are required to submit a word document with a short description of the method used in the quantification of uncertainties, as well as the method for calculating the sensitivity coefficients (if any). The file should be named *Userxx_UQ_method.doc* and include the main reasoning behind the selection of the uncertainty sources, the propagation method and a clear statement on how the uncertainty bands were constructed (e.g. ±2σ in the case of probabilistic methods).

11. RANKING THE SUBMMISIONS ACCORDING TO SPECIFIC MEASURES

To generate a ranking for the submissions, it is necessary to establish a measure that account for: the difference between calculated and experimental mean values, uncertainty level of the CFD simulations and the proper shape of the required profiles. These constrains impede the use of a linear measure, such as the one used in the previous OECD-PANDA benchmark, which is given by

$$M = \frac{1}{N_{data}} \sum_{i=1}^{N_{data}} \left| S_i - E_i \right| \tag{4}$$

where S_i and E_i represent the simulated and experimental values respectively, and N_{data} the total number of data points used in the analysis. If we take for example the velocity profile shown in Fig. 8, it can be seen that the flat uniform velocity profile (blue line) would lead to a lower value for *M* compared to the red profile. However, the red velocity profile is of a higher physical significance than the uniform profile. Another important

issue to note is that in this benchmark exercise, the comparison between simulations and experiments must also account for uncertainty bands (which should be provided by each participant). Submission without uncertainty bands **will not be considered** for the final synthesis report.

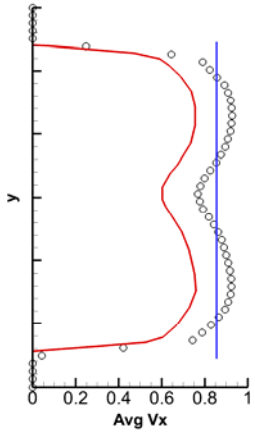

Figure 8. Schematic comparison between two simulated velocity profiles (continuous lines) and experiments (symbols).

Depending on the type of the UQ method used by each participant, the uncertainty band could be related to a certain quantile of a probability density function (output), to an interval (min, max) or to a member function (fuzzy variable). Therefore, a standardized measure that accounts for all these possibilities becomes highly complex. In order to simplify the analysis, a unique measure—based on a Gaussian distribution—is proposed. Let us imagine that the experimental and simulated values are represented by two Gaussian distributions—each characterized by a mean and standard deviation—then a normalized measure of the overlapping between the two distributions would indicate how close the simulations and experiments are.

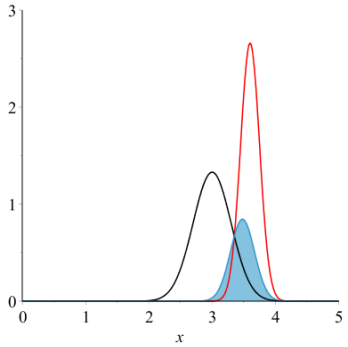

Figure 9. Schematic representation of the overlapping degree density ω (fidelity density) between two Gaussian distributions (filled blue).

We define then the degree of overlapping or fidelity of the numerical simulations by

$$\Omega = \int_{-\infty}^{\infty} \omega(x)dx \tag{5}$$

$$\omega(x) = \frac{1}{2\sigma_{sim}\sqrt{\pi}} \exp\left\{-\frac{1}{4}\left[\left(\frac{x-\mu_{\exp}}{\sigma_{\exp}}\right)^2 + \left(\frac{x-\mu_{sim}}{\sigma_{sim}}\right)^2\right]\right\} \tag{6}$$

where the $\omega(x)$ is the fidelity density (overlapping degree), and the subscripts *sim* and *exp* stand for simulation and experiment. The fidelity Ω will reach a maximum value—equal to 1—when the mean values of the two distributions coincide and the standard deviation of the simulations goes to zero (Fig. 10c). That means the maximum value will be reached only when the uncertainty in the simulations is zero and the simulations coincide exactly with experimental points. Increasing the uncertainty in the simulations or having different mean

values, will lead to a fidelity less than one. That is, Ω is bounded to the interval $\Omega \in [0,1]$. When using a measure such as the one defined in Eq. (5), a simulation with a mean value close to the experimental one and with a narrow uncertainty band, can have a fidelity Ω higher than that of a simulation with a broader uncertainty band with the mean value coinciding exactly with the experimental one (see Fig. 10). Hence, simulations with large uncertainty bands or with mean values far from the experimental one, will be penalized naturally in the calculation of Ω.

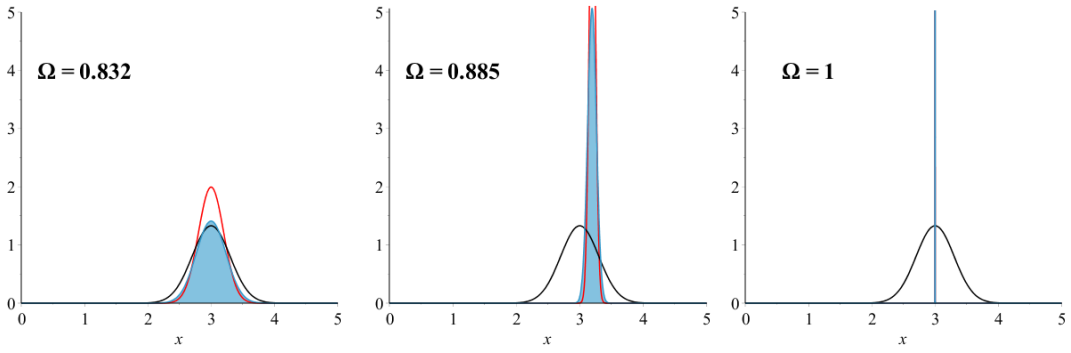

(a) (b) (c)

Figure 10. Overlapping degree Ω between simulations (continuous red) and experiments (continuous black). (a) The mean value of the simulations coincides with the experimental one and the CFD uncertainty band is slightly narrower than that of the experiment. (b) The mean value of the simulations is slightly different than the experimental one, but the CFD uncertainty is much less than the one observed in the experiments. (c) The CFD uncertainty is zero and the simulated variable coincides with the mean value from the experiment.

To standardize the procedure, the uncertainty bands provided by the participants **will be associated** to $\pm 2\sigma_{sim}$ in the Gaussian distribution representing the CFD results. In case the CFD uncertainty bands are not symmetric respect to the mean value, half of the difference between the upper and lower bands will be used to calculate the standard deviation of the simulations, that is

$$2\sigma_{sim} = \frac{(Upper - Lower)}{2} \tag{7}$$

The mean value μ_{sim} will be the one provided by the participants. The fidelity Ω will then be calculated at each grid point along all profiles for concentration, velocity and turbulence kinetic energy (see Fig. 4 for the location of the profiles). To evaluate the correctness of the shape of the profiles, we will make use of piecewise high order spline interpolation, and calculate the profiles derivatives at each grid point from the fitting curve *f*. Thus, at each grid point we will evaluate the correctness of the profiles' shape based on the relative error between the derivatives calculated from CFD and experimental results, that is

$$\mathrm{E} = \left| 1 - \frac{df_{sim}}{dy} \Big/ \frac{df_{\exp}}{dy} \right| \tag{8}$$

The fitting of the experimental and numerical profiles, as well as the calculation of the local derivatives, will be carried out by PSI in an automated manner. The final global correctness measure will be given by a combination of Ω and E, which is expressed as

$$M = \frac{1}{N_{data}} \sum_{i=1}^{N_{data}} \{\alpha(1-\Omega_i) + \beta \mathrm{E}_i\} \tag{9}$$

where the subscript *i* refers to i-th grid point and N_{data} to the total number of data points used in the analysis. The weighting factors α and β will be disclosed together with the experimental data for blind test. The best

simulations will have the lowest *M* scores. The measure defined in Eq. (9) will be used for velocity, turbulence kinetic energy and concentration. Since the transport of a scalar field (i.e. temperature and/or concentration) during a mixing process if the most important physical phenomena from a safety point of view, an additional measure is stablished to evaluate the accuracy of the simulations in predicting the concentration field. From the five concentration profiles submitted by the participants, we will extract—in an automated manner—the thickness of the mixing layer and compare it with the experimental values. The measure for the mixing layer thickness is defined as

$$M_C = \frac{1}{5}\sum_{i=1}^{5}\left|\delta_i^{\exp} - \delta_i^{sim}\right| \tag{10}$$

Raking tables will be generated for each individual measure (four in total).

12. CONCLUDING REMARKS

Organizing Committee

Arnoldo Badillo, Paul Scherrer Institute (PSI), Switzerland
Domenico Paladino, Paul Scherrer Institute (PSI), Switzerland
Dominique Bestion, Commissariat à l'Energie Atomique (CEA), France
Yassin Hassan, Texas A&M University, USA
Ghani Zigh, US Nuclear Regulatory Commission, USA
H.M. Prasser, Paul Scherrer Institute (PSI), Switzerland
Martin Kissane, OECD Nuclear Energy Agency, France (Secretariat)

Schedule

30 June	2015	PSI distributes Initial Benchmark Specifications (for Comment)
15 Aug.	2015	All participants must have sent any comments/queries on specifications to PSI
28 Aug.	2015	PSI issues final specifications
30 Sep.	2015	Deadline for registration to the benchmark
30 May.	2016	All participants must have sent their results to PSI (this is NOT extendable)
14 June	2016	Open benchmark meeting and release of test data
13 Sept.	2016	PSI presents the benchmark synthesis at CFD4NRS-6 Workshop
April	2017	Meeting on synthesis of post-test analyses

A6.3 Submittal Procedures

In order to be able to efficiently handle and compare calculated and measured data, all participants are requested to adhere STRICTLY to the formatting requested in this document. Datasets not conforming to the specified norms will be returned to participants for correction.

The deadline for submission of code predictions is set for May 30, 2016. Earlier submissions will be very welcome, and will considerably ease the burden on the organisers. Later submissions **will not be accepted** (no exemptions). Only **one submission per registered participant** will be accepted**.**

A special dropbox will be created on the PSI ftp site to which participants will be able to upload their results. Details will be distributed once the webpage is functional. Individual usernames and passwords will be allocated by the site manager and all data sets will be regarded as confidential. Unrestricted access to the data will only be available to the benchmark organisers. After uploading, participants are advised to download their datasets and compare with the originals to ensure that perfect transmission has been accomplished. Each participant will have the opportunity to exchange the datasets submitted for newer versions, but only up to the time of the deadline (May 30, 2016) at which time no further access to the dropbox will be possible. After the test data are opened at the Open Benchmark Meeting in June 2016 (actual date to be announced). Additionally, participants will thereafter **not be permitted to withdraw** their submissions.

Participants are free to repeat their calculations once they have the test data, and display any new results at the special Poster Session at the CFD4NRS-6 Workshop, as desired. However, only the *blind* code predictions will be considered for the synthesis.